Study on Unloading-wet Swelling Mechanism of Upper Arch Deformation of Mudstone Subgrade in a High-speed Railway

Xing Chen[1,2], Erping Zhao[1], Qi Liu[1*], Zihan Chen[2], Li Dang[3]

[1] Key Laboratory of Geological Hazards on Three Gorges Reservoir Area, Ministry of Education, China Three Gorges University, Yichang City, Hubei Province, 443002, China
[2] River Basin Hub Operation Management Center, China Three Gorges Corporation, Yichang City, Hubei Province, 443133, China
[3] Gezhouba power plant, China Yangtze power co., LTD, Yichang City, Hubei Province, 443002, China
* Corresponding author, e-mail: liuqi@ctgu.edu.cn

Abstract

Mudstone subgrade may exhibit rather complicated deformation behavior under the coupling effect of unloading and wet swelling caused by subgrade excavation. To study the deformation mechanism of mudstone subgrade, mudstones were sampled from the NO.3 branch tunnel of Badong section of Zhengzhou-Wanzhou High-speed Railway and a series of unloading and wet-swelling tests were carried out on them. We studied the long-term deformation behavior of mudstone subgrade caused by excavation based on a creep test with unloading conditions. The expansion rate of the complete mudstone cylinder samples was extremely low under the wetting and drying cycle, while that of the soil samples after the disintegration of complete mudstone was between 1% and 10% when immersed in water. Excavation unloading damage, groundwater infiltration, long-term creep deformation, dry-wet cycle, and hot-cold alternation catalyzed each other, leading to the aggravation of mudstone disintegration and the obvious increase of expansibility of underwater mudstone after disintegration. The maximum arch deformation of mudstone subgrade can be divided into three parts: the rebound deformation during short-term excavation, the creep deformation related to time and the wet-swelling deformation. Generally, the creep deformation would not converge in two years if support measures were not taken, the wet-swelling deformation could tend to a steady value after a certain period of excavation.

Keywords

mudstone, upper arch, unloading, wet swelling, mechanism

1 Introduction

Unlike the conventional normal speed railway construction, the standard of high-speed railway construction is much higher. The safe operation of the high-speed railway subgrade requires that the deformation of the subgrade should be controlled within millimeter level, and the adjustment space of the ballastless track for upper arch deformation is only 4 mm [1]. In recent years, the high-speed railway built-in soft rock areas have experienced the subgrade arch deformation after construction and operation. For example, since the second double line of Lanzhou-Xinjiang high-speed railway was opened and operated in December 2014, several continuous deformation sections of subgrade were found in the Jiayuguan section from 2014 to 2018, and some cushion plates have been adjusted to the limit. Through the analysis of measured data, it was found that 27 sections had subgrade deformation greater

than 10 mm, including 12 sections with the deformation of the upper arch greater than 26 mm, and the maximum deformation is 52.5 mm [2]. After the completion of the basic track laying of the Chengdu-Chongqing high-speed railway, when the track near the station yard of Neijiang North Railway Station was finely adjusted, the construction unit found that the ballastless track elevation of No. 2 cutting in this station was about 20 mm higher than the maximum design arch elevation [3]. The arch deformation of high-speed railway subgrade in mudstone areas has become a neck problem that restricts the construction and safe operation of high-speed railway lines.

At present, a large number of scholars have carried out theoretical research on the deformation of mudstone subgrade. In order to reveal the mechanism of time-dependent upper arch deformation of red-bed soft rock subgrade,

Zhong et al. [4] established the layered deformation mechanism model of red-bed soft rock subgrade and analyzed the short-term, medium-term, and long-term deformation mechanism and characteristics of subgrade from the perspective of the swelling test of red-bed soft rock and creep test under different hydraulic conditions, based on a specific deformation site of red-bed soft rock with deep excavation cutting subgrade upper arch deformation in southwest China, combined with the results of ground stress test, suction swelling test of red-bed soft rock and creep test under different hydraulic conditions. Wang et al. [5] studied the upper arch displacement and the response characteristics of the subgrade expansion under three working conditions (bed bottom, mudstone subgrade, bed bottom, and mudstone subgrade) with different swelling rates through the numerical simulation of the rail arch problem of high-speed railway ballastless track. Wang et al. [6] took a typical transition section subgrade swelling site as an example, determined the track arch and subgrade expansion layer by the on-site monitoring and the laboratory test and studied the influence of subgrade bed expansion on the transition section of the subgrade structure based on the numerical simulation. Wang et al. [7] selected six typical subgrade arching sites for field sampling and analyzed the swelling, soluble salt content, and mineral composition of subgrade soil and subgrade filler. Wang et al. [8] believed that the expansion process of expansive rock was a rheological process based on the swelling test results of expansive rock in Nanning-Kunming Railway.

For high-speed railway based on the cutting type mudstone roadbed and the tunnel type mudstone roadbed, the subgrade is under unloading stress condition after excavation. The mechanical properties of rock mass under excavation unloading conditions are essentially different from those under loading conditions [9–10]. Furthermore, the arch deformation of mudstone subgrade is a long-term complex physical and chemical change process under water and stress release [11]. Therefore, results acquired from traditional loading tests and swelling tests cannot sufficiently explain the arch deformation of the high-speed railway subgrade caused by mudstone unloading-wet swelling deformation. Instead, studies on the subgrade materials subjected to unloading and wetting should be carried out to achieve a more comprehensive understanding of the deformation mechanism of subgrades. For this purpose, typical mudstones were sampled at the No. 3 branch tunnel of Badong section of Zhengzhou-Wanzhou high-speed railway and a series of unloading and wet swelling tests were carried out to explore the deformation behavior of the mudstones.

2 Geological conditions

The No. 3 branch tunnel of Badong section of Zhengzhou-Wanzhou high-speed railway was excavated in 2019, as shown in Fig. 1. The surrounding rock was sprayed at the initial stage, and the concrete was poured into the bottom plate with a thickness of about 20 cm. In 2021, the project research team carried out field reconnaissance. The floor did not deform from the entrance but then began to deform from the inner tunnel. The deformation length was 235.87 m, and the floor uplift was up to 30 cm, shown in Fig. 2. Further forward, with the turning of the tunnel, the deformation position was transferred from the center of the tunnel section to the right sidewall. After the complete turning, no deformation occurred until the connection with the main tunnel. The ①, ②, ③, and ④ shown in Fig. 1 represent different sampling locations and lithologic regions. The deformation area of the subgrade is mainly concentrated in sections ② to ③.

In order to study the causes of the deformation of the upper arch of the No. 3 construction branch tunnel, some excavation work was carried out in this area. The

Fig. 1 The location of the No. 3 branch tunnel and the main tunnel of the Badong Section of Zhengzhou-Wanzhou High-speed Railway

(a)   (b)

Fig. 2 The photo of the interior of No. 3 branch tunnel; (a) Upper arch deformation, (b) Subgrade excavation

excavation results showed significant lithologic differences between the un-deformation area near the main tunnel and the deformation area. The un-deformation area is mainly gray marl, and the deformation area is mainly red mudstone. At the turning point, the right sidewall (to the tunnel) is red mudstone, and the left sidewall is gray marl. Therefore, the deformation is mainly concentrated in the right sidewall. Due to the lithologic differences, it can be considered that that the red mudstone of the Triassic mainly controls the deformation.

Through geological field survey, the correctness of this understanding is determined. The corresponding parts of the field are gray marl, and the lower part is red mudstone, shown in Fig. 3. The mineral composition is different between the grey marl and red mudstone. Gray marl is mainly composed of calcium carbonate, and mudstone is mainly composed of clay minerals and silty quartz. The clay minerals (such as kaolinite, illite, and montmorillonite) are the material basis for the expansion of red mudstone, which are generally aluminosilicates with layered or chain crystal lattices. The clay minerals have strong hydrophilicity due to their particular cellular structure, which can adsorb a large number of water molecules and cause bulk expansion.

After cutting the subgrade floor, the mudstone sample block is excavated. During the excavation, much mudstone has disintegrated into the soil, and only a small amount of large mudstone blocks can be obtained. The mineral composition analyses of the mudstone are shown in Figs. 4 and 5. The clay content of the sample is 20 %, the montmorillonite content in clay minerals is 0, and the illite content is 57 %.

3 Unloading creep experiment
3.1 Test scheme
The obtained mudstone blocks were processed into standard cylinder samples with a diameter of 50 mm and a length of 100 mm. In order to maintain the moisture content of mudstone, the standard cylinder sample was prepared and quickly wrapped with plastic film.

For soft rock such as mudstone, the excavation unloading deformation has prominent time-dependent characteristics. For tunnel subgrade, the stress field after excavation is characterized by the first principal stress increasing and the third principal stress decreasing [12]. For the cutting subgrade, the stress field after excavation shows that the first principal stress is unchanged, and the third principal stress gradually decreases [12]. Therefore, two test schemes were designed: Scheme I is the creep test scheme of increasing axial pressure and unloading confining
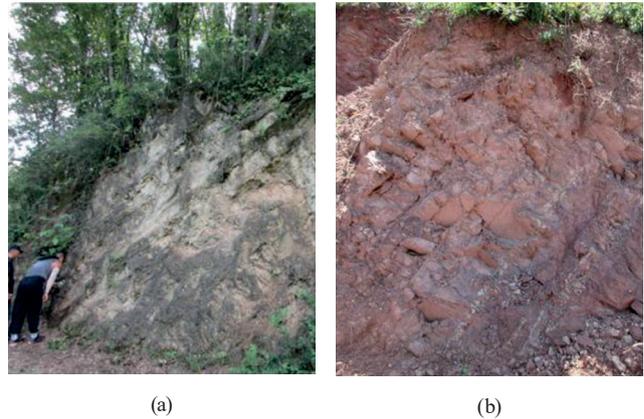

(a)   (b)

Fig. 3 The Gray marl and red mudstone seen in outcrops; (a) Gray marl, (b) Red mudstone
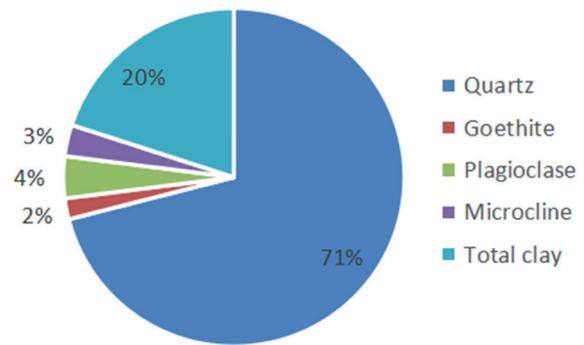

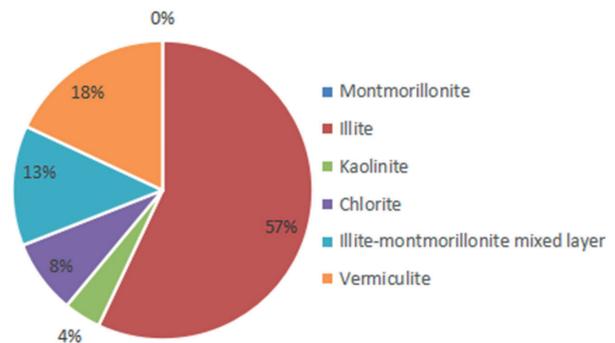**Fig. 4** The mineral composition of mudstone

Fig. 5 The relative content of clay minerals

pressure. Scheme II is the creep test scheme of constant axial pressure and unloading confining pressure. The test was carried out on the RLW-2000 Rock Triaxial Creep Tester, shown in Fig. 6, and the ambient temperature of the whole test was maintained at (20 ± 2) ℃.

Scheme I: (1) According to the hydrostatic pressure conditions, the loading rate of 0.05 MPa/s was applied to the predetermined value of 10 MPa gradually; (2) When the confining pressure was loaded to the predetermined value, the confining pressure remains constant, and the axial stress was loaded to the set stress level at the same loading rate continuously (about 70% of the ultimate
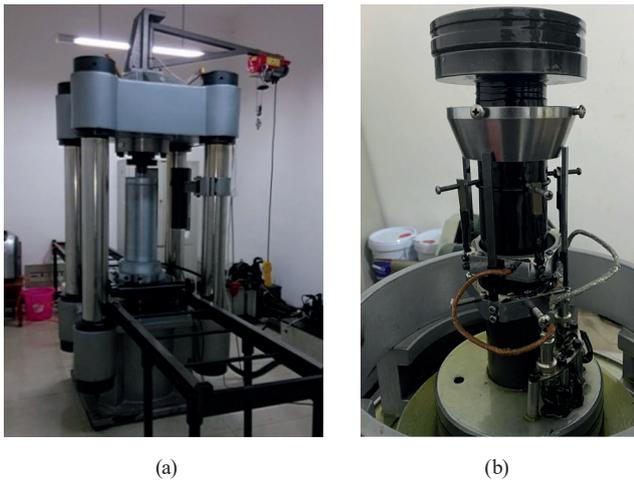
Fig. 6 The RLW-2000 rock triaxial creep tester; (a) The instrument, (b) Sample installation

compressive strength under the triaxial compression test with the same confining pressure); (3) The confining pressure was unloaded step by step at the rate of 0.05 MPa/s, and the axial compression was increased step by step with the same rate. The axial strain, lateral strain and time were recorded during the stage. When the creep deformation of the sample reached stability, the confining pressure was unloaded to the next level until the rock mass fails.

Scheme II: The first two steps of the scheme were the same as Scheme I, but it was different from Step (3). The unloading method in Step (3) of the scheme was to keep the axial compression constantly and unload the confining pressure at the rate of 0.05 MPa/s step by step.

3.2 Experiment results and analyses

Fig. 7 and Fig. 8 are the creep test curves of Scheme I and Scheme II, respectively. When the confining pressure of scheme I is unloaded to 4.5 MPa, and the confining pressure of Scheme II is unloaded to 3.5 MPa, the mudstone enters the accelerated creep stage, and the mudstone sample ruptures.

For Scheme I (increasing axial pressure and unloading confining pressure), the lateral strain of mudstone is obviously less than the axial strain. For the scheme II (constant axial pressure unloading confining pressure), the lateral strain and axial strain of mudstone are equivalent roughly. The creep deformation curve characteristics of the two schemes show that it has an obvious influence on the axial deformation of rock samples with the increase in axial stress during the increasing axial pressure and unloading confining pressure tests, and the lateral expansion effect of mudstone is more obvious during the constant axial pressure and unloading confining pressure tests.
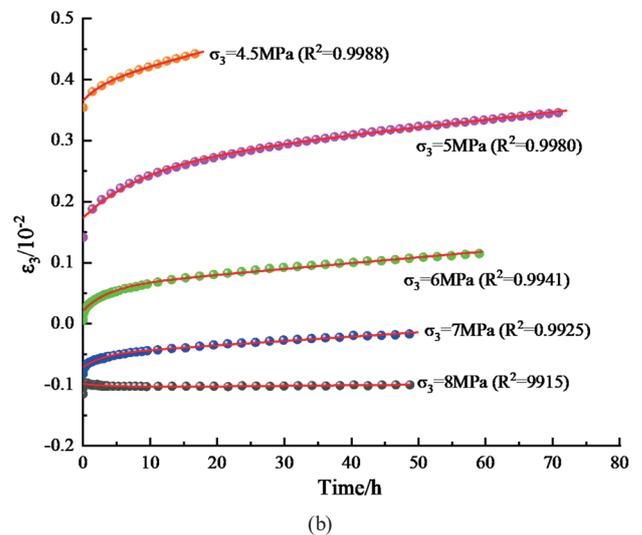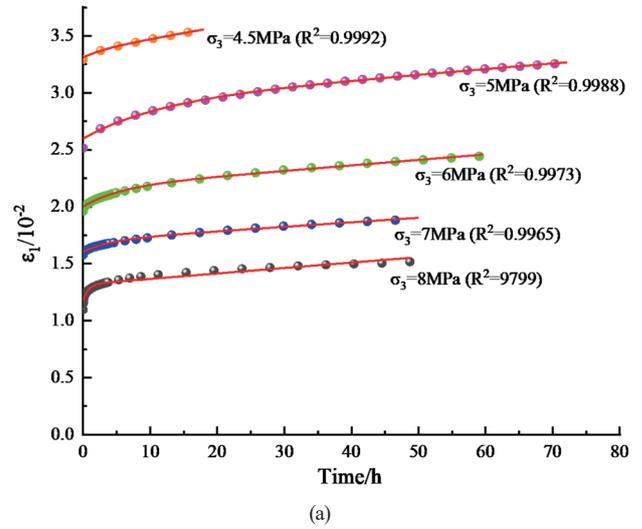

Fig. 7 The creep test curves of Scheme I; (a) Axial deformation, (b) Lateral deformation

The model includes elastic elements because the creep curve has instantaneous deformation at the starting point. In the steady creep stage, with the increase of time, the strain also increases accordingly, so the model contains viscous components. Many creep models describe viscoelasticity, such as the generalized Kelvin model and Burgers model. Given more numerical analysis software such as FLAC3D built-in Bergs model, considering the Burgers model for data fitting, Burgers model element combination as shown in Fig. 9:

Strain equation in Burgers model is:

$$\varepsilon = \frac{\sigma}{E_1} + \frac{\sigma}{\eta_1}t + \frac{\sigma}{E_2}\left(1 - e^{-\frac{E_2}{\eta_2}t}\right), \tag{1}$$

where t is the time. E_1 and E_2 are elastic modulus. η_1 and η_2 are viscous coefficients.

(a)

(b)

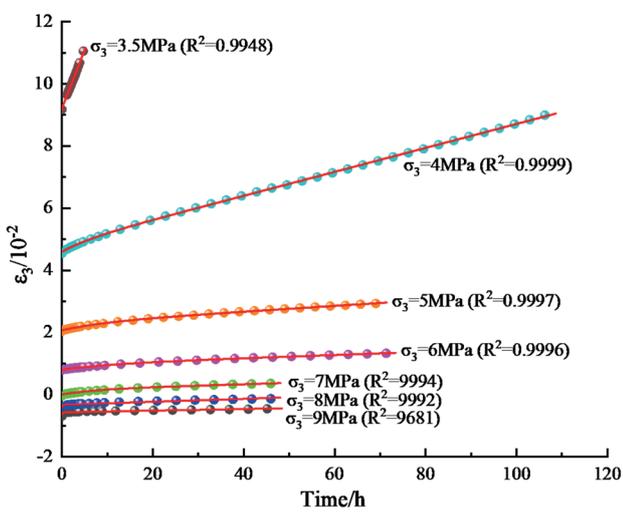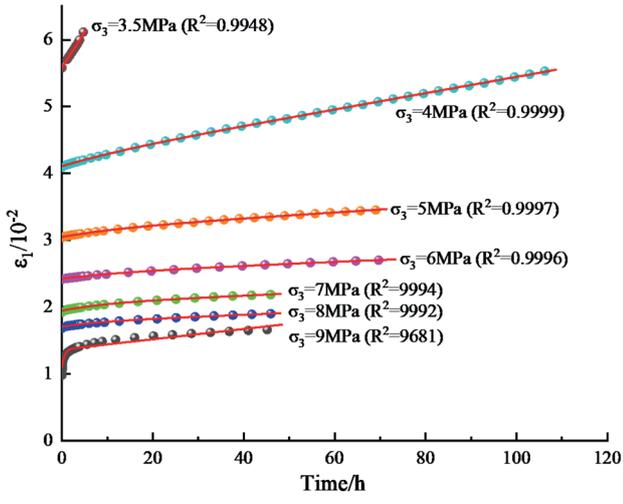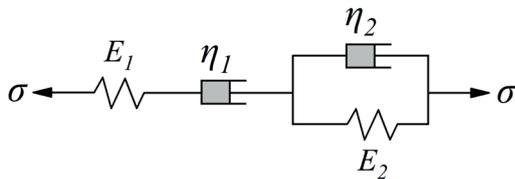**Fig. 8** The creep test curves of Scheme II; (a) Axial deformation, (b) Lateral deformation

Fig. 9 The Burgers model

The Burgers model was used to fit the creep test curve, and the fitting curve of the model was in good agreement with the test point. Four undetermined parameters E_1, E_2, and η_1, η_2, can be obtained by Origin fitting software, as shown in Table 1.

4 Wet swelling test

4.1 Swelling test of complete mudstone samples

Since the groundwater is abundant in the mudstone occurrence environment, the mudstone subgrade may be in the

Table 1 The Burgers Model Parameters of Scheme II

Confining pressure	5.0MPa	4.0MPa	3.5MPa
E_1/MPa	622.71	890.60	1107.00
E_2/MPa	46.61	807.74	4076.34
η_1/(GPa·h^{-1})	32.14	236.87	341.12
η_2/(GPa·h^{-1})	10.35	88.40	157.33

Fig. 10 The swelling test of complete mudstone Sample

dry-wet alternate environment. The dry-wet cyclic swelling test of the complete mudstone sample under lateral constraints was carried out, shown in Fig. 10.

As shown in Fig. 11, the results of multiple wetting-drying cycles confirm the following conclusions: The swelling rate of mudstone tends to zero in the first wet swelling test; With the increase of dry-wet cycles, the maximum swelling rate can reach 0.5%; From the change process of the mean value, the swelling rate of intact mudstone shows a change law of first increase and then decrease. The complete mudstone sample disintegrates after the seventh dry wet cycle, as shown in Fig. 12.

The SEM results of intact mudstone samples under different wetting-drying cycles show that: compared with natural samples, a certain number of large pores appear in the samples under three wetting-drying cycles, and a small number of loose particles separate; When the dry-wet cycle reaches six times, the internal cracks in the mudstone are rich and increasing, and the precipitation of clay particles increases, as shown in Fig. 13. The main reason for mudstone swelling is the high content of hydrophilic clay minerals. In the dry-wet cycle test of intact mudstone samples (before sample disintegration), the microcracks produced in the early dry-wet cycle provide a channel for hydration between clay minerals and water, and clay particles form water film after absorbing water, so the swelling
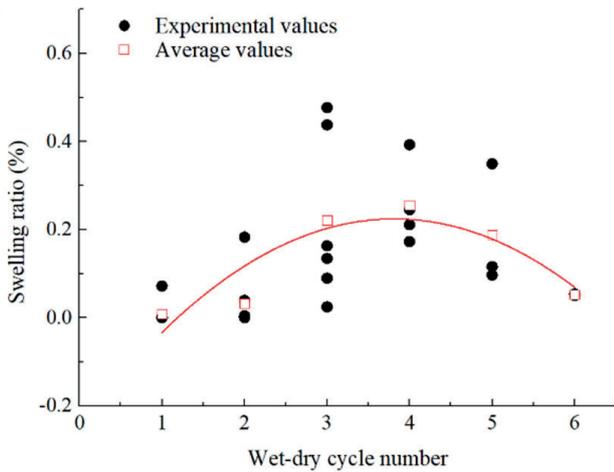
Fig. 11 The Mudstone swelling rate under dry-wet cycle

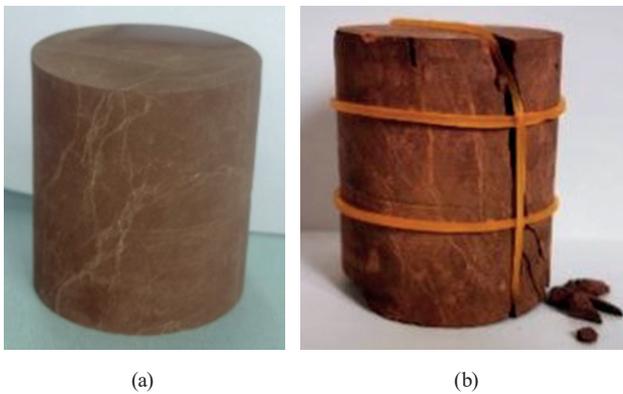(a)   (b)

Fig. 12 The photos before and after rock sample disintegration; (a) Before dry wet cycle, (b) After the seventh dry wet cycle

of intact mudstone is enhanced. With the increase of drying and wetting cycles, the mudstone skeleton continuously loses the clay mineral particles, and the cohesive force becomes weaker than before. Due to the decrease of clay mineral content, the swelling rate of intact mudstone samples decreases.

4.2 Swelling test of soil samples
Although the maximum swelling rate of intact mudstone can reach 0.5% after dry-wet cycles, it is still at a deficient level. Considering that many mudstones have been disintegrated into the soil, some soil samples were made and the swelling rate test was conducted.

The wet swelling test of complete mudstone samples is carried out under the condition that no external load is applied. If the upper load is applied, the swelling of mudstone will be limited. According to the "Code for Geotechnical Test of Railway Engineering" (TB10102-2010), the vertical swelling deformation tests of soil samples under six kinds of upper loads with lateral confinement,
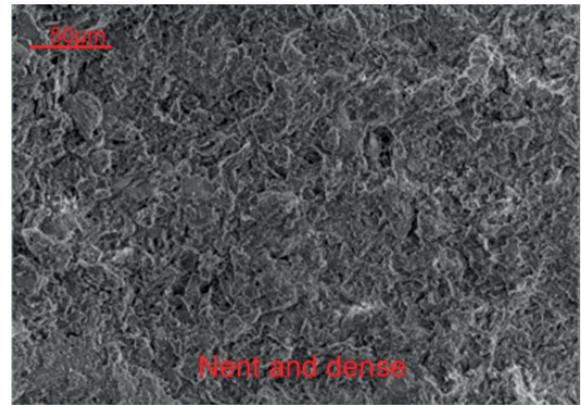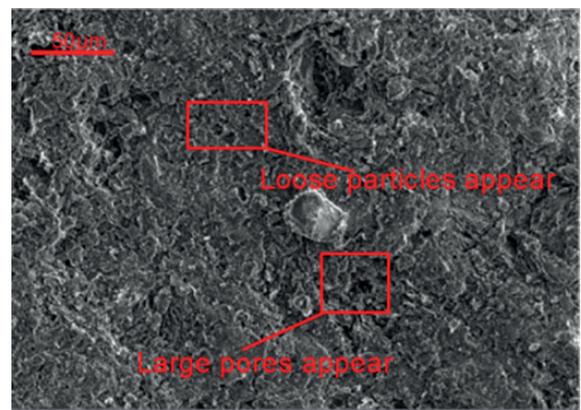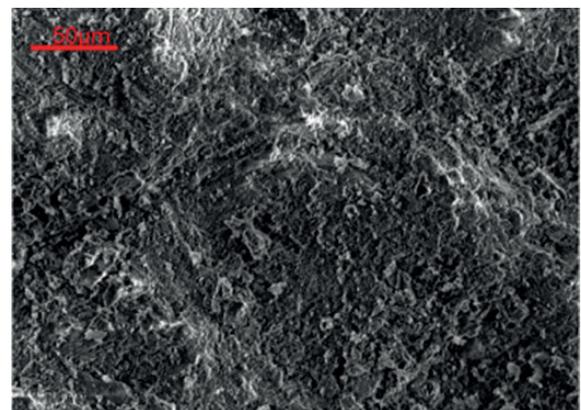
Fig. 13 The Microstructure characteristics of intact mudstone; (a) Natural sample, (b) After three wet-dry cycles, (c) After six wet-dry cycles

namely, 0 kPa, 10 kPa, 20 kPa, 30 kPa, 40 kPa and 50 kPa (the swelling force of undisturbed samples is about 45 kPa in a laboratory test, and the upper loading value is designed based on this) after immersion [13].

The test equipment adopts GDS triaxial consolidation apparatus as shown in Fig. 14, and the remodeling sample is a cylinder with a diameter of 61.8 mm and a height of 20 mm.
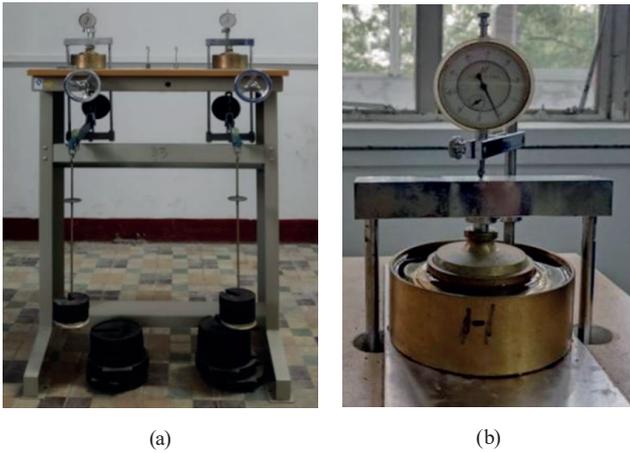
(a)   (b)

Fig. 14 The GDS consolidation tester; (a) The instrument,
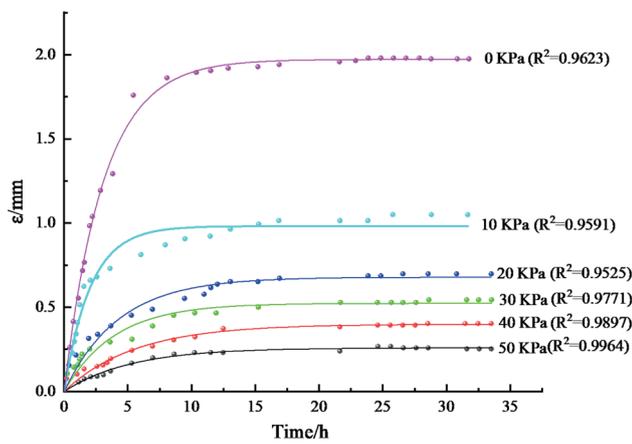(b) Sample installation

Fig. 15 The swelling curve of mudstone under different loading
conditions

The swelling curve of mudstone under different loading conditions is shown in Fig. 15. The swelling rate results of soil samples are between 1% and 10%, which is quite different from the swelling rate of intact mudstone samples.

The Microstructure characteristics of soil samples are shown in Fig. 16. In the process of deformation of soil samples in case of water, the structural change is divided into two parts: First, the existing cracks provide water flow path, and the water seepage in the existing cracks of the sample is rapid; Second, the particles with weak cementation around the crack collapse under the damage of water, and the bearing capacity of the structure is lost.

For the wet swelling model of mudstone, previous studies have proposed the swelling force model [14], the humidity stress field theory [15] (using the thermal swelling of the temperature field instead of the humidified swelling of the humidity field), there is also water swelling creep model [1]. The swelling deformation of mudstone has a significant time effect, similar to the creep
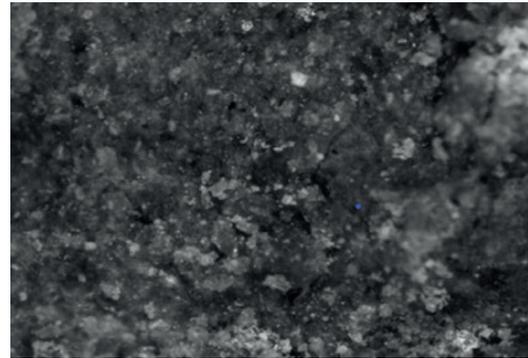
(a)
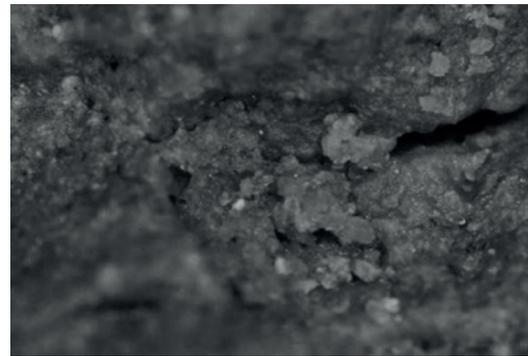
(b)
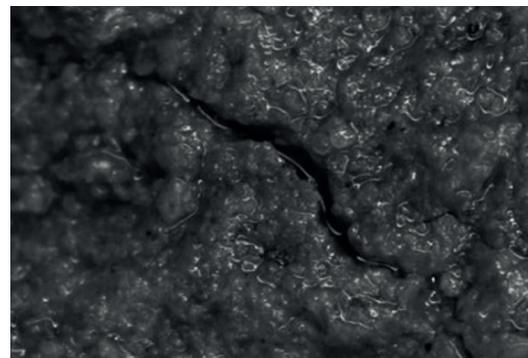
(c)

Fig. 16 The Microstructure characteristics of soil samples [13];
(a) Natural sample, (b) Unsaturated sample, (c) Saturated sample

process of rock under load. Referring to the element model of rock creep, according to the characteristics of discrete points in the test, the swelling deformation of the starting point is generally zero, so we considered using a similar Kelvin model with a series of elastic and viscous elements, as shown in Fig. 17.

The equation of the similar Kelvin model is:

$$\varepsilon = K\left(1 - e^{-\eta \cdot t}\right), \tag{2}$$

where t is the time. K and η are the fitting parameters. When t tends to be large enough, K is a constant value, and the physical meaning of parameter K is the final
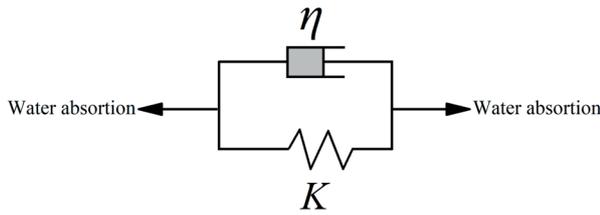
Fig. 17 The Kelvin creep model of mudstone swelling

stable swelling deformation value. Parameter η is regarded as the coefficient related to the water absorption swelling viscosity.

The fitting curve of the model was in good agreement with the test curve. Two undetermined parameters K and η can be obtained by Origin fitting software, as shown in Table 2.

If the swelling coefficient of mudstone without upward load is K_s, the swelling coefficient of mudstone is a decreasing function of upward load under stress conditions. Based on the Huder-Amberg model [11], we can propose the expression of swelling coefficient K under stress conditions:

$$K = K_s \left[1 - \lambda \cdot \lg(1 + \sigma_3) \right], \tag{3}$$

where K_s is the stable swelling strain value without upper load, that is, when $\sigma_3 = 0$, $K = K_s$. λ is the model parameter obtained by fitting the discrete point $K - \sigma_3$ of the wet swelling test under the condition of loading on the same type of mudstone samples.

As shown in Fig. 18, $\lambda = 0.4968$ is obtained by fitting the relationship curve between K and σ_3 in Table 2, and the data correlation is about 99.9%, indicating that the established mudstone swelling constitutive model has good applicability.

5 Mechanism of mudstone disintegration

The moisture swelling of intact mudstone is not significant, and the maximum moisture swelling of soil samples with the disintegration of intact mudstone can reach 10%. Therefore, we can infer that the disintegration degree of mudstone greatly influences the swelling. The mechanism of mudstone disintegration is:

1. The excavation unloading leads to the decrease of the minimum principal stress and the increase of the maximum principal force in the stress environment
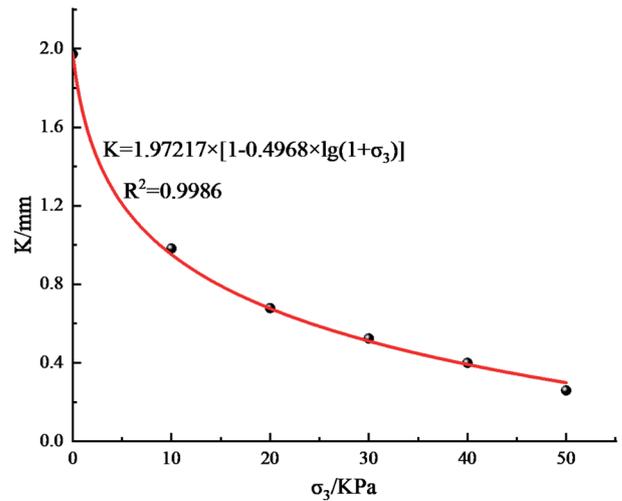

Fig. 18 The Relationship between stable swelling strain value and overlying load

of mudstone. The unloading damage causes a large number of microcracks (or damage) in the mudstone.

2. The groundwater of Badong tunnel is rich. After excavating the branch tunnel, the surrounding rock gradually releases the shallow stress, and if forms the stress difference between the deep high-stress area and the shallow stress area of the surrounding rock. The groundwater quickly seeps out near the excavation face. The unloading effect produces microcracks that provide seepage channels for groundwater. At the same time, the seepage effect leads to the further erosion of mudstone particles around the microcracks, the outflow of water, and the further swelling of microcracks.

3. Mudstone belongs to soft rock with prominent creep aging characteristics. During the operation period of the No. 3 branch hole of Badong tunnel for 2 years, the creep deformation of shallow mudstone in the subgrade continues to increase, and the creep deformation leads to further cracks.

4. Dry-wet cycles and alternating cold and heat lead to weathering, swelling, shrinkage of mudstone, and lots of rock fractures.

The above various interactions are catalysts for each other, leading to the aggravation of mudstone disintegration. After disintegration, the mudstone formed the soil sample, and the swelling performance is significantly increased.

Table 2 The Kelvin model parameters of mudstone swelling with different loading conditions

Load	50 KPa	40 KPa	30 KPa	20 KPa	10 KPa	0 KPa
K/mm	0.25962	0.40004	0.52435	0.67892	0.98221	1.97217
η/(mm·h^{-1})	0.19190	0.17978	0.25450	0.23383	0.48489	0.32431

6 Mechanism of upper arch deformation of mudstone subgrade

For the high-speed railway, the upper arch of the subgrade is the coupling result of unloading and swelling:

1. During the construction period, the redistribution stress field is produced after the subgrade excavation. The the redistribution stress field shows unloading in the vertical direction with loading in the horizontal direction for tunnels. And the vertical upward rebound deformation is ε_1. During operation, since the mudstone belongs to typical soft rock, which easily leads to creep deformation, upward rebound deformation develops further. The creep rebound deformation is recorded as ε_2.

2. Mudstone contains clay minerals that are generally aluminosilicates with layered or chain crystal lattices, such as montmorillonite, illite, and kaolinite. Due to its unique cell structure, and the strong hydrophilicity of clay minerals, it can absorb many water molecules, and water molecules enter between the cells, thus changing the distance between the cells, which is macroscopically manifested as volume swelling. The swelling of these three clay minerals is in the order of montmorillonite > illite > kaolinite. The mudstone swelling deformation is recorded as ε_3. The swelling force is less than the external load pressure for the deep part of the mudstone subgrade, and the swelling deformation can be ignored. Due to the unloading effect of the shallow surface after excavation, the upper coating load is small, and the swelling force is greater than the external load pressure. The resulting swelling deformation is ε_3.

3. As shown in Fig. 19, the total deformation formula of the upper arch of mudstone is $\varepsilon = \varepsilon_1 + \varepsilon_2 + \varepsilon_3$. ε_1 is short time excavation rebound deformation, generally independent of time; ε_2 is the creep deformation related to time. According to the unloading creep Burgers model derived above, the creep rebound increases with time. If the necessary engineering treatment measures are not taken, the displacement may still not converge within two years of operation. ε_3 is wet swelling deformation, according to the previous derivation of the wet swelling Kelvin model. After a certain period (a day or so), the swelling tends to the limit then stops growing.

4. Due to the effects of the dry-wet cycle and cold-hot alternation, the negative dry shrinkage deformation ε_4 may be generated. The dry shrinkage deformation may make the total deformation of the upper arch fluctuate around the overall trend in a specific range. The dry shrinkage deformation is not considered when calculating the maximum upper arch deformation.

7 Conclusions

The arch deformation of mudstone subgrade is a long-term complex physical and chemical change process under the combined action of water and stress release. In this paper, a series of unloading and wet swelling experiments were carried out to study the deformation behavior of mudstone sampled from the No. 3 construction branch tunnel in Badong section of Zhengzhou-Wanzhou high-speed railway. The conclusions are as follows:
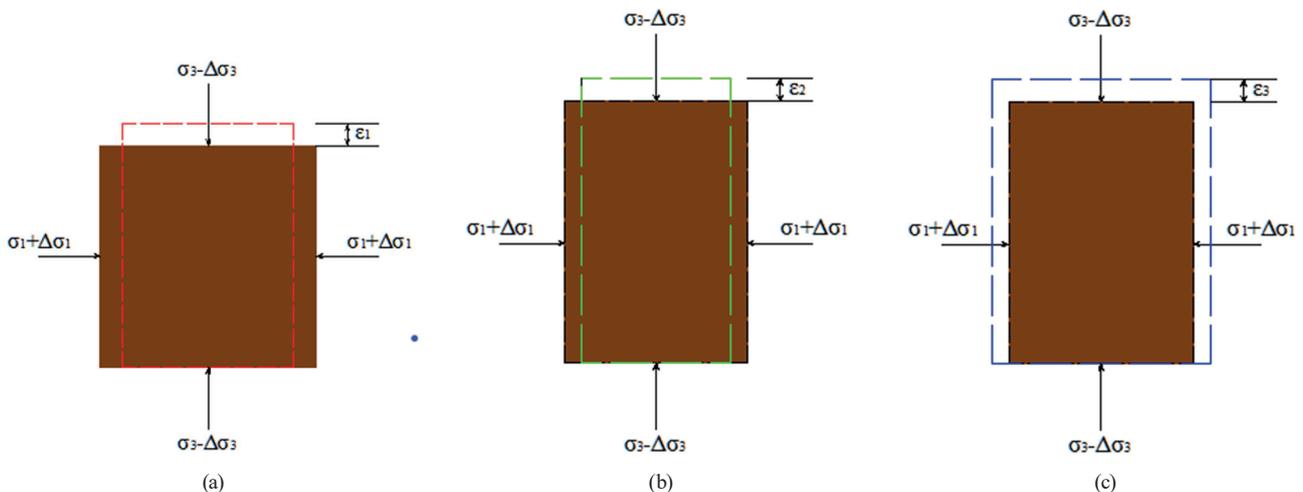

Fig. 19 Decomposition diagram of arch deformation on mudstone roadbed; (a) Short-term excavation unloading deformation, (b) Long-term unloading creep deformation, (c) Wet-swelling deformation

1. A creep test of intact mudstone cylinder specimen was carried out by unloading the confining pressure and loading the axial pressure to simulate the long-term deformation behavior of tunnel excavation under unloading deformation. It was found that the Burgers constitutive model can be used to fit the test data.

2. The swelling rate of the intact mudstone samples was at an extremely low level under dry-wet cycles; the immersion swelling rate of the soil samples was between 1 % and 10 %, which was significantly increased compared with the intact mudstone sample. The excavation and unloading caused the aggravation of mudstone disintegration, groundwater permeability, long-term creep deformation, dry-wet cycle, cold-hot alternation, and other effects, leading to the weathering, swelling, and contraction of mudstone. The above effects contributed to the aggravation of mudstone disintegration. After disintegrating, the expansion of mudstone in water increased significantly.

3. It was found in the swelling test that the larger the upper load, the smaller the stable swelling strain value of mudstone. Referring to the creep element, the Kelvin constitutive model can reasonably simulate the wetting process of mudstone.

4. The maximum total deformation of the upper arch of mudstone subgrade can be decomposed and expressed by the formula $\varepsilon = \varepsilon_1 + \varepsilon_2 + \varepsilon_3$, where ε_1 is the rebound deformation of short-term excavation, which is generally independent of time; ε_2 is the creep deformation related to time; ε_3 is the wet swelling deformation. With the extension of time, the creep rebound continues to increase. If the necessary engineering treatment measures are not taken, the displacement may still not converge within two years of operation. After a certain period (about one day), the swelling does not increase after reaching the limit value.

Conflicts of interests
The researcher claims no conflicts of interests.

References

[1] Zhong, Z.-B., Li, A.-H, Deng, R.-G, Wu, P.-P, Xu, J. "Experimental study on aging swelling and deformation characteristics of red-bed mudstone in central Sichuan", Chinese Journal of Rock Mechanics and Engineering, 38(1), pp. 76-86, 2019. (in Chinese)
https://doi.org/10.13722/j.cnki.jrme.2018.0861

[2] Jing, X.-X. "Analysis on the Deformation Causes of the Upper Arch of the Subgrade of a Section of the Lanxin Second Double Line and Research on the Remediation Measures", MSc Thesis, Lanzhou Jiaotong University, 2019. (in Chinese)
https://doi.org/10.27205/d.cnki.gltec.2019.001300

[3] Yang, J.-X., Ma, X.-C., Liu, Q.-R. "Discussion on the problem of the upper arch of the Chengdu-Chongqing high-speed railway", Railway Architecture, 59(8), pp. 112–115, 2016. (in Chinese)
https://doi.org/10.3969/j.issn.1003-1995.2016.08.28

[4] Zhong, Z.-B., Li, A.-H., Deng, R.-G., Wu, P.-P., Wang, K., Chen, M.-H., Fu, Z.-Q. "Study on time-dependent upheaval deformation mechanisms of red-bed soft rock subgrade of high-speed railways", Chinese Journal of Rock Mechanics and Engineering, 39(2), pp. 327–340, 2020. (in Chinese)
https://doi.org/10.13722/j.cnki.jrme.2019.0423

[5] Wang, R., Cheng, J.-J., Li, Z.-G., Wang, M.-T., Ma, Y.-L. "Research on the response characteristics of track overshoot caused by subgrade swelling", Chinese Journal of Railway Science and Engineering, 16(12), pp. 2942–2950, 2019. (in Chinese)
https://doi.org/10.19713/j.cnki.43-1423/u.2019.12.006

[6] Wang, M.-T., Wang, R., Cheng, J.-J., Li, Z.-G., Gao, L. "Research on the arching law of ballastless track induced by swelling of subgrade bed in the transition section of road and bridge", Chinese Journal of Railway Science and Engineering, 18(3), pp. 645–652, 2021. (in Chinese)
https://doi.org/10.19713/j.cnki.43-1423/u.T20200416

[7] Wang, P.-C, Yao, J.-K., Chen, F., Zhang, Q.-L. "Experimental research on the cause of overhanging of ballastless track subgrade", Railway Architecture, 58(1), pp. 43–46, 2018. (in Chinese)
https://doi.org/10.3969/j.issn.1003-1995.2018.01.10

[8] Wang, X.-N., Han, H.-Z., Wen, J.-Q. "The coupled effect of swell and rheology for the slope engineering of swelling rock", Journal of Geological Hazards and Environment Preservation, 8(4), pp. 33–39, 1997. (in Chinese)

[9] Li, J.-L. "Unloading Rock Mass Mechanics", China Water Resources and Hydropower Press, Beijing, China, 2003. ISBN 9787508416212, (in Chinese)

[10] Li, J.-L., Wang, L.-H. "The principle and application of unloading rock mechanics", Science Press, Beijing, China, 2016. ISBN 9787030463067, (in Chinese)

[11] Steiner, W. "Swelling rock in tunnels: Rock characterization, effect of horizontal stresses and construction procedures", International Journal of Rock Mechanics and Mining Sciences and Geomechanics Abstracts, 30(4), pp. 361–380, 1993.
https://doi.org/10.1016/0148-9062(93)91720-4

[12] Li, J.-L., Chen, X., Dang, L., Dong, Y.-H., Cheng, Z., Guo, J. "Triaxial unloading test of sandstone after high temperature", Chinese Journal of Rock Mechanics and Engineering, 30(8), pp. 1587–1595, 2011 (in Chinese)

[13] Ma, L.-N. "Study on the swelling mechanism and influence of low-clay mineral mudstone in high-speed railway subgrade", PhD Thesis, Lanzhou Jiaotong University, Year. (in Chinese)

[14] Liu, J.-Y. "Study on the swelling mechanism and development law of mudstone", PhD Thesis, China Academy of Railway Sciences, Year. (in Chinese)

[15] Xue, Y.-J. "Research on deformation test and calculation model of upper arch of mudstone subgrade of high-speed railway", MSc Thesis, Lanzhou Jiaotong University, Year. (in Chinese)